Proceedings of the Canadian Society for Mechanical Engineering International Congress 2021
CSME Congress 2021
June 27-30, 2021, Charlottetown, PE, Canada

Approximations for use in cycling thermodynamic systems: Applications for Stirling engines

Steven M.W. Middleton[1] and David S. Nobes[1*]
[1]Mechanical Engineering Department, University of Alberta, Edmonton, Alberta
*dnobes@ualberta.ca

Abstract—A pair of approximations are presented which are useful for the solving of cyclic single-phase sub-sonic compressible thermodynamics machines with particular relevance to Stirling engines. The first approximation models compressible, acoustics neglected flows in a constant pressure volume. This approximation has similar performance to implicit incompressible techniques and when applied to the modelling of a laboratory low-temperature Stirling engines can model a variety of running conditions with an average error on thermodynamic power of 23%, ranging between 5% and 42%. The second approximation is designed to accelerate the convergence of the wall temperatures towards steady-state conditions. This technique was shown to converge 2-3 orders of magnitude faster than the baseline physics when applied to a large low-temperature engine.

Keywords – thermodynamic, numerical, dynamic, approximation

I. INTRODUCTION

Low-temperature engines are a poorly understood classification of Stirling engines (SEs), which in itself is much less understood than other forms of heat engines. Interest in Stirling engines has emerged as a result of the recent push towards renewable resources. Some renewables, such as low-temperature geothermal sources feature hot temperatures on the order of the boiling point of water, a cold temperature in the realm of developed power generation technologies. However, such thermal sources are so common that the province of Alberta, Canada, has enough of this low temperature geothermal to reasonably produce 600MW [1]. Yet, the entire country of Canada has yet to produce a single geothermal power plant. At large enough scales technologies which use turbines such as organic Rankine cycle (ORC) are superior to reciprocating devices like SEs, but turbines become less economical to produce at smaller scales [2]. At these scales Stirling engines may have higher efficiencies [3] than ORCs in addition to reduced corrosion or toxicity by nature of inert working fluids such as nitrogen, helium or hydrogen. With enough development, engines forgo the mechanism altogether, becoming free-piston engines which require no lubrication or maintenance for decades even when running at full power [4].

Natural Sciences and Engineering Research Council of Canada
Alberta Innovates Energy and Environmental Solutions
Terrapin Geothermics
University of Alberta Future Energy Systems grant.

With regards to the numerical modelling of SEs, approximations of the pressures and therefore power within an engine can be easily obtained via the Schmidt model, as created by Gustav Schmidt [5]. The Schmidt model was described and expanded by Urieli and Berchowitz [6] who created the equation set for adiabatic analysis in their SIMPLE model. Their formulation served as the basis for a series of models up until the CPMS model [7], or Comprehensive Polytropic Model of Stirling engines. The trend in model improvements is notably in the direction of greater detail with regards to the influences of the wall temperatures into the solution. Farther into the design process it is beneficial to include even greater detail than the analytical models can handle. The logical step to accomplish this simply is to discretize the engine into finite elements.

When solving a system of elements, the physics involved can be approached in one of two ways. The entire cycle can be calculated at once, acknowledging that the start and end points at steady-state must be the same. This is often very efficient to accomplish by multivariable non-linear solving algorithms [8]. Alternatively, the cycle can be iterated through time, ultimately approaching a steady-state value in a similar manner to which the true system does so [9]. The nature by which this is accomplished can be quite revealing to the operation of the process. The later will be of discussion here, selected due to its ability to predict transient behavior and facilitate the addition of new features with relative simplicity. The first of approximations presented in this paper will discuss the formulation of an iterative scheme for solving for the gas flow rates within a SE. This and the acceleration method following it were created for implementation into MSPM a modular single-phase model for Stirling engines and other reciprocating devices [10].

II. STIRLING ENGINE PROCESSES

A SE undergoes a cycle of heating, expansion, cooling and compression once per rotation. This process, with regards to a gamma type engine, is shown below in Figure 1.

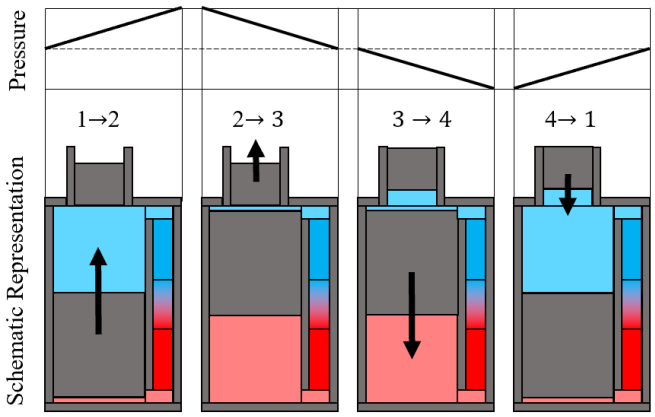

Figure 1. Ideal Stirling enigne cycle, from left to right: (1→2) bulk heating creating rise in pressure, (2→3) engine expands extracting work from increased pressure, (3→4) bulk cooling creating drop in pressure, (4→1) engine compresses extracting work from decreased pressure.

As a heat engine, SEs are subject to the Carnot limit of efficiency equal to $1 - T_C/T_H$ whereas T_C is the gas temperature during compression and T_H is the gas temperature during expansion. The ideal cycle is physically impossible, subject to the constraints of heat transfer, flow losses and the practicalities of mechanism design. Controlling the divergence from the ideal cycle of a SE is fundamentally about the control of two things: pressure and heat transfer.

A. *Pressure*

The correlation of high pressures during expansion and low pressures during compression is what drives a SE. These pressure changes are induced via changes in the volume and average temperature of the engine contents. This temperature change is significant and does not happen uniformly across the engine resulting in substantial variances in density within the engine. Pressure losses are significant through the heat exchangers and regenerator structures, owing to the balance between high temperature change against incurred pressure losses. Pressure losses, though dependent on temperature through its weak relationship to viscosity are strongly related to engine speed and pressurization.

B. *Heat Transfer*

Thermally, a SE has two optimum operating conditions: one where there is no heat transfer outside of the heat exchangers and one where heat exchange is perfect. These are formally known as the adiabatic and isothermal idealizations [6]. A real engine will operate somewhere in-between these points. In reality, most engines exhibit adiabatic behavior [6], thus any tendency for heat transfer outside the heat exchangers will result in a divergence from the adiabatic ideal, lowering the power. The quantity of energy exchanged with the walls is dependent on the wall temperatures, this value is minimum when the walls have reached steady-state conditions. Thus, if an engine has been preheated beneficially it will run very well for a period of time as the walls act as additional heat exchange surface. If an engine is started from cold, then the walls will reduce the temperature difference, reducing the engines power until the walls are at steady-state. Changes in load will induce similar transients in SEs as the engine reaches a new operating point.

III. Approximating Compressible Gas Interactions at Low Speeds

The following is a derivation of a flow rate solving algorithm for low speed gas interactions. A summary and explanation of the assumptions within this approximation are as follows:

(a) Uniform pressures everywhere – Stirling engines in particular are characterized by the absence of venting and normally do not include valves into their operation. At low speeds, such as the case with large low-temperature SEs the pressure-drop and kinetic energy is ideally very low. The flow is still compressible however but not at speeds where acoustic effects effect the engine operation. If a gas volume is at rest then it will have equal pressures everywhere (in the absence of gravity effects). It can be assumed that for low enough speeds this tendency also applies.

(b) Ideal gas equation of state – Stirling engines typically avoid phase change and operate on inert gases well removed from their condensation or critical temperatures and pressures.

(c) One dimensional flow – The majority of important processes occur within the fine structures of heat exchangers and regenerative structures with relatively high ratios of length to hydraulic diameter. Making this assumption prevents the accurate modelling of recirculation, bends, entrance effects, jet impinging and preferential flows. However, by modelling as a pipe network it significantly reduces the computational burden.

(d) Low mechanical acceleration – Stirling engines, if designed for a power generating purpose, must yield relatively steady rotational rates over the cycle. Thus, when modelling such engines, even under transient scenarios it is assumed that the acceleration is small relative to the speed.

(e) Kinetic and potential energy of the gas is ignored, due to the low density, speed and vertical distance change of low temperature Stirling engines.

The flow rates may be solved by solving for the flow rates such that a future point $(t+\delta)$ is also at uniform pressures as below:

$$P_{i,t+\delta} = P_{j,t+\delta} = m_{i,t+\delta}RT_{i,t+\delta}/V_{i,t+\delta} = m_{j,t+\delta}RT_{j,t+\delta}/V_{j,t+\delta} \quad (1)$$

The pressure P is defined at two elements (i & j) which are connected to each other. The pressure, assuming an ideal gas can be calculated from the mass (m), specific gas constant (R), temperature (T) and volume (V). By making the assumption that the specific gas constant is constant throughout it can be removed from the equation. These variables are expanded in the following subsections.

A. Volume ($V_{i,t+\delta}$)

If the engines dynamics are known, the value of $V_{i,t+\delta}$ is known. The dynamics can be known by assuming that the engine is kinematic and of constant velocity, or by allowing the acceleration of the engine to lag behind by a small increment. This lag can be as small as one timestep or span several timesteps. For example in the MSPM model [10], the cycle is divided into precalculated points at set angular positions. The gas interactions are simulated while engine speed evolves between two predefined points. The initial speed is the speed at the end of the previous timestep, the final speed is a result of accelerating the initial speed using the forces applied in the previous increment.

B. Mass ($m_{i,t+\delta}$)

The final mass of an element is a product of the mass flow in an out of that element. This is formalized in (2).

$$m_{i,t+\delta} = m_{i,t} + \delta\sum y_{fc,i,t}\dot{V}_{fc}\rho_{fc,i,t} \quad (2)$$

The variable $\dot{V}_{fc}$ is the volumetric flow rate at an interface between elements spanning the timestep. The sign convention variable $y_{fc,i}$ is positive if a positive value of $\dot{V}_{fc}$ would result in a flow into element i, and is negative otherwise. The variable $\rho_{fc,i,t}$ is the density as measured at the interface at the start time.

C. Temperature ($T_{i,t+\delta}$)

The final temperature must be determined from an energy balance. It is assumed that the gas is ideal and by this assumption the change in temperature is proportional, by the constant volume heat capacity (c_v), to the change in specific internal energy (u):

$$T_{i,t+\delta} = T_{i,t} + du_i/c_{v,i} \quad (3)$$

The change in internal energy is expanded, here the variables are represented in their true form to be approximated later as either the value at t or $t+\delta$:

$$du_i = (dU_i - u_i\, dm_i)/m_i \quad (4)$$

Here, kinetic and potential energy is ignored. Thus, the change in total internal energy (dU_i) is equal to the sum of heat flow (dQ_i) (heat transfer and transported internal energy) and work (δW_i) (flow work and boundary work) produced by the element. As an unsteady-flow process.

$$dU_i = dQ_i - \delta W_i \quad (5)$$

The heat transfer component is easily calculated using the interactions the element has with its neighbors. Interactions which depend on the flow conditions (for example the Nusselt number via convection) can be approximated by the flow conditions determined during the previous timestep. The energy which is transported is proportional to the flow rates, thus the heat transfer can be approximated as:

$$dQ_i = dQ_{cond,i} + \delta\sum y_{fc,i}\dot{V}_{fc}\rho_{fc}u_{fc} \quad (6)$$

The variable $dQ_{cond,i}$ represents the heat flow via conduction entering the element i during the timestep. The work acting on the element is totaled from the flow and boundary work acting on the element.

$$\delta W_i = P_{i,t}dV_i - \delta\sum y_{fc,i}\dot{V}_{fc}P_{fc,t} \quad (7)$$

Thus, (5) is approximated as:

$$dU_i = dQ_{cond,i} + \delta\sum y_{fc,i}\dot{V}_{fc}(\rho_{fc,t}u_{fc,t} + P_{fc,t}) - P_{i,t}dV_i \quad (8)$$

Substituting (8) and (4) into (3) and approximating u as $u_{i,t}$ and m as $m_{i,t+\delta}$ gives:

$$T_{i,t+\delta} = T_{i,t} + (Q_{cond,i} + \delta\sum y_{fc,i}\dot{V}_{fc}\rho_{fc,t}(u_{fc} - u_i + P_{fc,t}/\rho_{fc,t}) - P_{i,t}dV_i)/(m_{i,t+\delta}c_{v,i,t}) \quad (9)$$

Note the distinction is made between the specific internal energy measured at the interface (u_{fc}) and that present in the element (u_i).

D. Bringing it all together

Substituting (2) and (9) in (1) and equating the value of m_i to $m_{i,t+\delta}$ gives the following:

$$(T_{i,t}m_{i,t} + T_{i,t}\delta\sum y_{fc,i}\dot{V}_{fc}\rho_{fc,t} + (Q_{cond,i} + \delta\sum y_{fc,i}\dot{V}_{fc}\rho_{fc,t}(u_{fc,t} - u_{i,t} + P_{fc,t}/\rho_{fc,t}) - P_{i,t}dV_i)/c_{v,i,t})/V_{i,t+\delta} = P_{j,t+\delta}/R \quad (10)$$

This equation can be solved for a network of connected elements via matrix inversion in the form $A\dot{V} = b$. Each row represents a pair of elements

$$g(i,fc) = y_{fc,i}\rho_{fc,t}(T_{i,t} + (u_{fc,t} - u_{i,t} + P_{fc,t}/\rho_{fc,t})/c_{v,i,t}) \quad (11)$$

$$f(i,fc) = (T_{i,t}\, m_{i,t} + \delta(Q_{cond,i} - P_{i,t}(V_{i,t+\delta} - V_{i,t}))/c_{v,I,t})/(\delta V_{i,t+\delta}) \quad (12)$$

The entry $A(a,b)$ would contain $g(i_a,fc_b) - g(j_a,fc_b)$ whereas i_a and j_a are the two elements included in row "a" with i_a is the element the flow leaving and j_a being the element the flow is entering. The function g will be zero if the element and interface do not interact. The entry b(a) would contain $f(i_a,fc_a) - f(j_a,fc_a)$ and the negatives of any g's which represent flow rates which are a known value. Networks which contain constant pressure elements can be simplified by having each element maintain a constant pressure. Networks which require more equations to solve, due to containing loops solve for flow rates by ensuring that approximated pressure drops are equal to zero when integrated over a loop.

IV. Predicting Steady-State Wall Temperatures

The use of an iterative scheme with a nodal approach to predict the steady-state behavior of a cycle with a large time-constant can result in many cycles having to be calculated. Or worse the returned result, due to an insufficiently small tolerance on convergence, may be far from the true steady-state of the device. The following represents an acceleration method for predicting the steady-state point of the solid components of the engine.

At steady-state the integral of heat flux to and from a solid element of the engine will be equal to zero, this rule ensures that the value of all elements will be equal at the start and end of a cycle. The instantaneous heat transfer to any element $Q_{in,i}(t)$ is equal to the following:

$$Q_{in,i}(t) = \sum C_{ij}(t)(T_j(t) - T_i(t)) \quad (13)$$

where C_{ij} is the thermal conductance of the interface between the elements i and j. All properties are subject to varying with time (t). Each temperature value can be reduced to steady $T_{i,avg}$ and unsteady $dT_i(t)$ terms. This appears as the following:

$$Q_{in,i}(t) = \sum C_{ij}(t)(T_{j,avg} - T_{i,avg} + dT_j(t) - dT_i(t)) \quad (14)$$

The integral over a single cycle will result in the following, in which the steady-components can be extracted from the integral:

$$\int Q_{in,i}dt = 0 = \sum((T_{j,avg} - T_{i,avg})\int C_{ij}(t)dt) + \sum(\int(C_{ij}(t)(dT_j(t) - dT_i(t)))dt) \quad (15)$$

Making assumptions can help to simplify this. Solid temperatures, due to their large thermal mass do not change significantly over a cycle. This is due to the difference in volumetric heat capacity of steel, a common construction material, and high-pressure air, for which at room temperatures and 10 bars of pressure still results in a 2 orders of magnitude difference in volumetric heat capacity. This error increases when less material is involved in the exchange.

This assumption causes a division between the conductance paths between two solid elements and those between a solid and gas element:

$$0 = \sum_{solid\text{-}solid}((T_{j,avg} - T_{i,avg})\int C_{ij}(t)dt) + \sum_{gas\text{-}solid}(\int C_{ij}(t)T_j(t)dt - T_{i,avg}\int C_{ij}(t)dt) \quad (16)$$

For the solid-solid case, in the case of kinematic devices, constant thermal conductance and low in-cycle speed variation the integral $\int C_{ij}(t)dt$ can be precalculated as a cycle average value $C_{ij,eff\text{-}solid}$. For gas-solid interactions the actual value of $C_{ij}(t)$ may vary significantly while the temperatures are being converged, requiring that the integrals be calculated from the results of the previous cycle. Ultimately, this results in the following definitions.

$$C_{ij,eff\text{-}solid} = \int C_{ij}(t)dt = 1/2\pi \sum C_{ij,\theta}\Delta\theta \quad (17)$$

$$C_{ij,eff\text{-}mixed} = \int C_{ij}(t)dt = (\sum C_{ij}\delta(t))/\sum\delta(t) \quad (18)$$

$$CT_{ij,eff\text{-}mixed} = \int C_{ij}(t)T_j(t)dt = (\sum C_{ij}T_j(t)\delta(t))/\sum\delta(t) \quad (19)$$

The complete equation can be assembled in matrix form $AT_i = b$ with each row corresponding to the interactions with a particular element. The main diagonal appears as $\sum C_{ij,eff\text{-}solid} + \sum C_{ij,eff\text{-}mixed}$ the sum of non-zero conductance values associated with the rows element. The non-diagonal spaces are symmetric with element at row i and column j containing the negative of the conductance between solid elements i and j. Within the vector b, the row i is composed of $\sum CT_{ij,eff\text{-}mixed}$ for each gas element j associated with solid element i. Solving this equation via matrix inversion yields approximate average temperatures for the solid elements. This matrix inversion yields an average value of temperature if the temperatures were completely static, they are not however completely static, but rather a superposition of the unsteady and steady or slowly evolving component.

The magnitude of the unsteady component is equal to the difference between the current value of temperature and the mean value. During convergence to steady-state the mean value will vary across a cycle. If this mean value is assumed to follow a linear trend the unsteady component can be approximated as the following:

$$dT_{i,0} = T_{i,0} - (T_{i,avg,measured} + \tfrac{1}{2}(T_{i,0} - T_{i,0,prev})) \quad (20)$$

The change in the mean value is approximated via the change in the starting temperature across the cycle. A few additional variables were introduced here: $T_{i,0}$ is the temperature measured at the current starting point, $T_{i,0,prev}$ was the recorded at the previous starting point last cycle. $T_{i,avg,measured}$ is the average value of temperature over the cycle. The new temperature $T_{i,new}$ is as follows:

$$T_{i,new} = A^{-1}b + dT_{i,0} \quad (21)$$

This formula activates once per cycle, with the intent of bringing the solid temperatures into line with the more quickly modified gas temperatures.

V. Results & Discussion

The following subsections test the effectiveness and accuracy of the approximations outlined in this paper.

A. Approximating Compressible Gas Interactions at Low Speeds

The model was compared against 12 tests conducted at steady-state on a low-temperature Stirling engine described by Stumpf [14]. The engine was designed to operate with a source temperature of 95 °C and sink temperature of 5 °C and had a normal operating speed of between 1-3 Hz, producing a shaft power between 6-8 Watts at peak operating conditions. The experimental results are from Nicol-Seto [15] and feature the engine operating using a series of drive mechanisms using elliptical gears which give the pistons dwelling or more linear motion profiles, having benefits as a challenging modelling problem. The approximation was implemented into MSPM alongside a turbulence handler inspired by the Stirling engine modelling software SAGE [8]. Calibration of the model was conducted only to correct the compression ratio as the actual engine features a compliant rubber bellow as its volume changing piston. A selection of 3 representative pressure-volume diagrams as well as a summary plot are included as

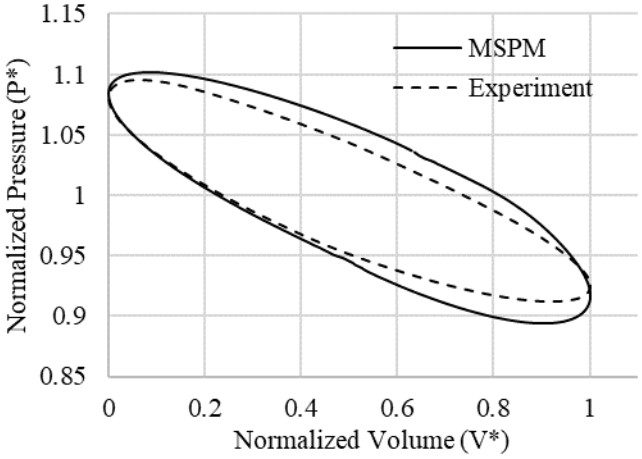

(a)

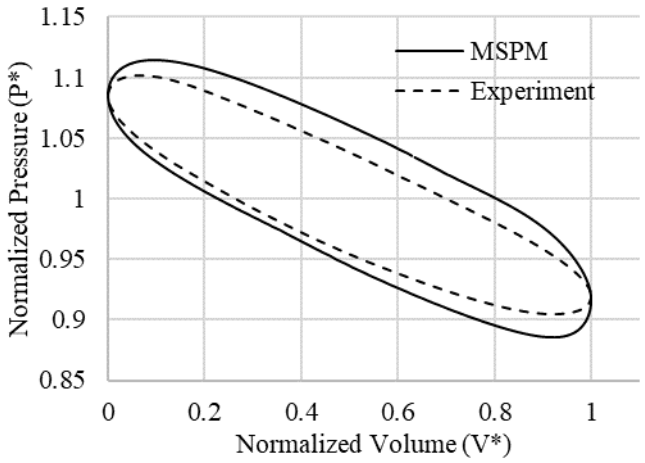

(b)

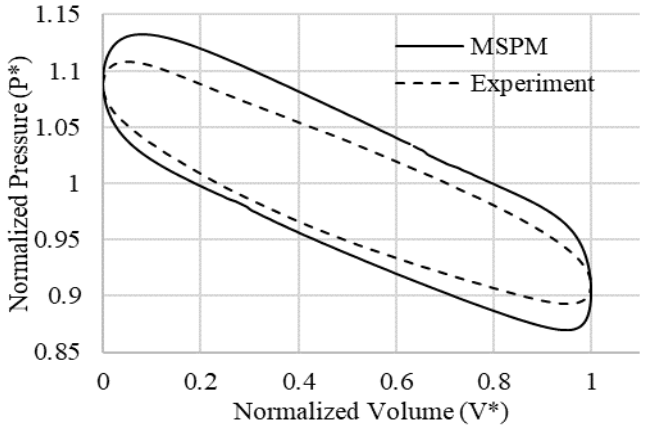

(c)

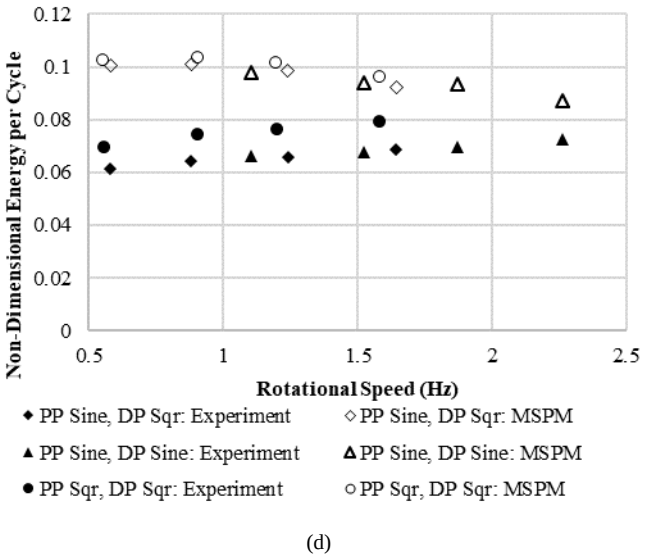

(d)

Figure 2. (a) Pressure-Volume plot of engine at 2.26 Hz with both pistons having sinusoidal motions, (b) engine at 1.644 Hz with a dwelling displacer and sinusoidal power piston motions, (c) engine at 1.58 Hz with both pistons having a dwelling motion, (d) summary of non-dimensional areas for all configurations.

The algorithm performed sufficiently well at the low speeds of the EP-1 engine. The model consistently overestimates the experimental results, with a trend of decreasing error towards medium speeds, which is observed in each set of 4 tests. This may be due to multiple factors, including the low performance of the friction and heat convection correlations in pulsatile situations. The set with the largest error is the set with a dwelling displacer piston and sinusoidal power piston with an average of 32% error in absolute thermodynamic power. In total the average error in cycle power is 23%. In using this model to determine trends the test with dual dwelling cycles created the largest area in both the experimental and numerical results with the other two tests falling onto the same line.

B. Predicting Steady-State Wall Temperatures

The presented algorithm was applied to MSPM, a numerical model which incorporates the pseudo-compressible scheme described in this paper. The convergence of this algorithm was compared against an unmodified algorithm. The results are shown in Figure 3.

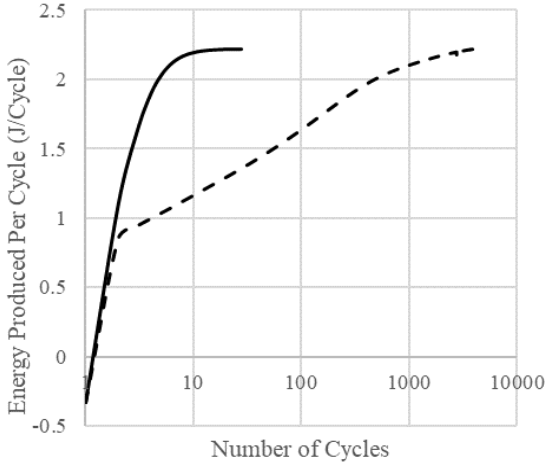

Figure 3. Comparison of accelerated (solid) vs native (dashed) convergence behaviour

It can be observed in Figure 3. that during the first 2 cycles both algorithms followed a similar trend. After which the accelerated algorithm continued towards steady-state and the unmodified algorithm slowed down. The sharp increase is due to the gas temperatures in the engine being established through the first passes through the heat exchangers. The remainder of the convergence period is the heating of the engine body, which takes a small, but noticeable amount of energy away from gas each cycle. When comparing total amount of cycles simulated the accelerated algorithm reached a tolerance of 2% within 9 cycles, while the unmodified algorithm reached this point after 2057 cycles, representing a roughly 2 orders of magnitude speedup. The computational cost of this algorithm is relatively small, with periodic data collections and once per cycle matrix inversions.

It should be noted that both simulations converged to exactly the same value within 0.2%, thus the approximation did not introduce a noticeable change in the outputted results.

VI. Conclusion

Approximations and optimizations give designers greater freedom to explore concepts, or invest in simulations of greater detail so long as the approximations are close enough to that which they model. This paper has presented a pair of approximations. The first mathematical derivation solved for the flow rates by assuming the pressure remained constant, this approximation allows larger timesteps than a compressible simulation would permit through the neglection of acoustics and by using an implicit formulation. This assumption produced results which matched up well against experimental tests resulting in an average error of 23% over a range of exotic piston motions and engine speeds.

An acceleration method was introduced which was applicable to iterative schemes. The presented algorithm allowed the simulation to converge to within 2% of the final value in 9 cycles. A simulation using an incremental heat transfer model converged to this same tolerance after 2057 cycles. This represents a substantial 2-3 orders of magnitude speedup while converging to the same final value.

VII. Further Improvements

The approximation of fine interactions is a potential area of improvement for iterative schemes. In Stirling engines these occur frequently as fine metal structures inside of heat exchangers and regenerators, with thickness scales consistently in the fraction of a millimeter. These can ultimately result in a severely limited timestep in particular when used with low-speed engines. The author is currently developing a method to use odes to represent the interactions.

Acknowledgment

The author would like to acknowledge the financial support of the Natural Sciences and Engineering Research Council of Canada, Alberta Innovates Energy and Environmental Solutions, Terrapin Geothermics and the University of Alberta Future Energy Systems grant.

References

[1] J. Banks and N. B. Harris, “Geothermal Potential of Foreland Basins: A Case Study from the Western Canadian Sedimentary Basin,” *Geothermics*, vol. 76, no. May, pp. 74–98, 2018.

[2] Michael A. Devine and Chris Lyons, “Engines? Turbines? Both? Choosing Power for CHP Projects,” no. August, p. 15, 2013, [Online]. Available: http://www.carolinacat.com/documents/choosing-power-for-chp-projects.aspx.

[3] I. Oma, “Potential of Stirling Engine and Organic Rankine Cycle for Energy Recovery in Ship Machinery Systems,” Norwegian University of Science and Technology, 2015.

[4] D. Zudell, “Stirling Converter Sets 14-Year Continuous Operation Milestone,” *NASA*, 2020. https://www.nasa.gov/feature/glenn/2020/stirling-convertor-sets-14-year-continuous-operation-milestone (accessed Jan. 27, 2021).

[5] G. Schmidt, “The Theory of Lehmann’s Calorimetric Machine,” *Z. ver. Dtsch. Ing.*, vol. 15, 1871.

[6] I. Urieli, “Stirling Cycle Machine Analysis,” *Russ College of Engineering and Technology Mechanical Engineering Department*, 2018. https://www.ohio.edu/mechanical/stirling/ (accessed May 09, 2018).

[7] M. Babaelahi and H. Sayyaadi, “Analytical closed-form model for predicting the power and efficiency of Stirling engines based on a comprehensive numerical model and the genetic programming,” *Energy*, vol. 98, no. April, pp. 324–339, 2016, doi: 10.1016/j.energy.2016.01.031.

[8] D. Gedeon, “Sage User ’s Guide. Sage v11 Edition,” 2016, [Online]. Available: http://www.sageofathens.com/Documents/SageStlxHyperlinked.pdf.

[9] S. K. Andersen, H. Carlsen, and P. G. Thomsen, “Numerical study on optimal Stirling engine regenerator matrix designs taking into account the effects of matrix temperature oscillations,” *Energy Convers. Manag.*, vol. 47, no. 7–8, pp. 894–908, 2006, doi: 10.1016/j.enconman.2005.06.006.

[10] S. M. W. Middleton, “A modular numerical model for Stirling engines and single-phase thermodynamic machines,” University of Alberta, 2021.

[11] R. Stirling, “Stirling air engine and heat regenerator,” 4081, 1816.

[12] E. ToolBox, “Steel Wool Grades,” 2010. https://www.engineeringtoolbox.com/steel-wool-grades-d_1619.html (accessed Jan. 28, 2021).

[13] J. Hensen and A. E. Nakhi, “Fourier and Biot numbers and the accuracy of conduction modelling,” in *Fourier and Biot numbers and the accuracy of conduction modelling*, 1994, no. January 1994.

[14] C. J. A. Stumpf, “Parameter Optimization of a Low Temperature Difference Gamma-Type Stirling Engine to Maximize Shaft Power,” University of Alberta, 2018.

[15] M. Nicol-Seto, “Investigation of Drive Mechanism Modification to Increase Thermodynamic Performance of a Low Temperature Difference Gamma Stirling Engine,” University of Alberta, 2021.

[16] B. Hoegel, D. Pons, M. Gschwendtner, A. Tucker, and M. Sellier, “Thermodynamic peculiarities of alpha-type Stirling engines for low-temperature difference power generation: Optimisation of operating parameters and heat exchangers using a third-order model,” *Proc. Inst. Mech. Eng. Part C J. Mech. Eng. Sci.*, vol. 228, no. 11, pp. 1936–1947, 2014, doi: 10.1177/0954406213512120.